

## Supporting information

# Revealing the Distinct Thermal Transition Behavior between PEGA-Based Linear Polymers and Their Disulfide Cross-linked Nanogels

Wenhui Sun,<sup>a</sup> Zesheng An<sup>\*b</sup> and Peiyi Wu<sup>\*a</sup>

**Materials.** 2-methoxyethyl acrylate (MEA, 98%) and poly(ethylene glycol) methyl ether acrylate (PEGA,  $M_n=480$ ) were received from Sigma-Aldrich. D,L-dithiothreitol (DTT, 99%) was obtained from Aladdin. 2,2'-azobisisobutyronitrile (AIBN, CP) purchased from Sinopharm Chemical Reagent was purified by recrystallization from ethanol. All monomers were passed through a column of  $Al_2O_3$  to remove the inhibitor before use. Pyridyl Disulfide Ethyl Acrylate (PDSEA) and PDMA<sub>35</sub> Macro-CTA were synthesized according to two previous reports, respectively.<sup>1-2</sup> All the other reagents were received from Sinopharm Chemical Reagent Co., Ltd.

**Characterizations.** Hydrodynamic diameters ( $D_h$ ) of nanogels (1 wt%) were measured on a Malvern ZS90 after being allowed to equilibrate at the setting temperatures for 2 min. <sup>1</sup>H NMR spectra were collected on a Bruker AV 500 MHz spectrometer with  $CDCl_3$  or  $D_2O$  as solvent. Gel permeation chromatography (GPC) was performed on a Waters Alliance e2695 GPC system, equipped with a Styragel guard column, a Waters

Styragel HR3 (molecular weight range  $5.0 \times 10^2$ – $3.0 \times 10^4$  g mol<sup>-1</sup>), a Waters Styragel HR4 (molecular weight range  $5.0 \times 10^3$ – $6.0 \times 10^5$  g mol<sup>-1</sup>), and a Waters Styragel HR5 (molecular weight range  $5.0 \times 10^4$ – $4.0 \times 10^6$  g mol<sup>-1</sup>). Detection was performed on a 2414 refractive index (RI) detector using *N,N*-dimethylformamide (HPLC grade, containing 1 mg mL<sup>-1</sup> LiBr) as the eluent at a flow rate of 0.8 mL min<sup>-1</sup>. The temperature of the columns was set at 65 °C and the temperature of the refractometer was set at 45 °C. Analysis of molecular weights and dispersities was performed using Empower 2 software against poly(methyl methacrylate) (PMMA) standards (molecular weight range  $2.4 \times 10^2$ – $1.0 \times 10^6$  g mol<sup>-1</sup>). The FTIR spectra of 10 wt% precursor polymers and nanogels in D<sub>2</sub>O collected during heating with an interval of 1 °C were selected to perform PCMW and 2D correlation analyses. Primary data processing was performed using the software 2D Shige ver. 1.3 (Shigeaki Morita, Kwansai Gakuin University, Japan). The contour maps were plotted using Origin Program 2 ver. 8.0 with red and yellow as the positive intensities and blue as the negative intensities. An appropriate window size ( $2m + 1 = 11$ ) was chosen to generate good-quality PCMW spectra. Variable-temperature <sup>1</sup>H NMR spectra of nanogel solutions were recorded on a Varian Mercury plus (500 MHz) spectrometer using D<sub>2</sub>O as the solvent (concentration = 10 wt%) at an increment of 1 °C.

### **Determination of Pyridothione Content**

To estimate the remaining amount of pyridine groups in the CL nanogel, the amount of pyridothione which is a byproduct during nanogel synthesis by disulfide bond formation was monitored via UV-vis, which were performed with samples taken at

predetermined time intervals. Once this was measured, we calculated the amount of pyridothione based on its known molar extinction coefficient ( $8.08 \times 10^3 \text{ M}^{-1}\text{cm}^{-1}$  at 343 nm).<sup>3</sup> The percentage of crosslinking was calculated by assuming that formation of a single, crosslinking disulfide bond would require cleavage of two PDS units and produce two pyridothione molecules. Based on the calculation of pyridothione molar concentration using the extinction coefficient, four different cross-linked nanogels by adding 10, 20, 40 or 50 mol % (against the precursor PDS groups) of DTT to the precursor polymer, whose remaining PDS groups were determined to be 84, 68, 31 or 12% (16, 32, 69 or 88 mol% of PDS groups were used in the crosslinking reaction). Because the total PDS composition of the polymer is 6.9%, we estimated that the crosslinking density corresponds to 0.6, 1.1, 2.4 or 3%.

### **Synthesis of PDMA-*b*-P(MEA-*co*-PEGA-*co*-PDSEA) Copolymers**

RAFT polymerizations with varied molar ratios of MEA: PEGA: PDSEA were carried out in DMF at 70 °C using PDMA<sub>35</sub> as a macro-CTA for block copolymer synthesis. The monomer concentration was controlled at 50% (w/v) and the molar ratio of AIBN/macro-CTA was controlled at 0.5: 1. The target degree of polymerization (DP) was ~530. Macro-CTA (0.074 g, 0.02 mmol), MEA (1.171 g, 9 mmol), PEGA (0.48 g, 1 mmol), and PDSEA (0.144 g, 0.6 mmol) were dissolved in 3.7 mL of DMF. The solution was degassed with nitrogen at 0 °C for at least 40 min before immersion into a preheated oil bath at 70 °C. After the temperature was stabilized, a degassed solution of AIBN (1.64 mg, 0.01 mmol) was injected via a microsyringe. The polymerization was allowed to continue under protection of nitrogen. The conversion of MEA, PEGA

and PDSEA monomers were calculated to be 49%, 96%, 67% for 24 h polymerization, respectively, as shown in Figure S1.  $M_{n,theory} = 59900$ ,  $M_n = 54300$  (GPC),  $M_w/M_n = 1.23$  (GPC)

### **Synthesis of Nanogel**

The precursor polymer ( $10 \text{ mg mL}^{-1}$ ) was dissolved in water and placed in a vessel pre-heated at  $60 \text{ }^\circ\text{C}$  for 20 min. When the polymer solution turned turbid, different amounts of DTT (10, 20, 40 or 50 mol% relative to PDS) was added. Addition of a deficient amount of dithiothreitol (DTT) into the solution of the precursor polymer upon heating would cause the cleavage of a well-defined percentage of the PDS groups to the corresponding thiol functionalities. These thiol functionalities will then react within the polymeric aggregates with unreacted PDS functionalities. This reaction results in disulfide cross-links within the polymeric aggregates, causing the formation of the nanogels. Then the mixture was stirred for 24 hours to allow for cross-linking. The resulting nanogel dispersion was purified by dialysis using a membrane ( $7000 \text{ g mol}^{-1}$ ).  $^1\text{HNMR}$  spectrum of the N-20 nanogels is shown in Figure S2.

### **Perturbation correlation moving window (PCMW)**

PCMW as a recently developed technique has basic principles which were first proposed by Thomas.<sup>4</sup> Then in 2006 Morita<sup>5</sup> improved this method to a wider range of applicability by introducing a perturbation variable into the correlation equation. Together with its ability to determine transition points, PCMW spectra can also be used

to monitor spectral variations along the temperature perturbations, combining the signs of synchronous and asynchronous spectra by the following rules: a positive synchronous correlation indicates spectral intensity increasing, while a negative one indicates spectral intensity decreasing; a positive asynchronous correlation shows a convex spectral intensity variation while a negative one shows a concave variation.<sup>5</sup> The transition temperatures can be easily deduced from the synchronous map and transition temperature regions can be clearly determined by peaks in asynchronous map.

Figure S3 illustrates the PCMW synchronous and asynchronous spectra of the PDMA-*b*-P(MEA-*co*-PEGA-*co*-PDSEA) precursor polymers in D<sub>2</sub>O during heating from 25 to 50 °C. The transition regions and points of different groups can be directly deduced from the PCMW spectra, from which we determined that the transition regions between 34.5 and 41 °C and VPTT is *ca.* 37 °C for all the bands related to CH and C=O groups. PCMW synchronous and asynchronous spectra of the P(MEA-*co*-PEGA-*co*-PDS)/PDMA nanogels are shown in Figure S4. They are generated from all the FTIR spectra during heating from 25 to 50 °C with an interval of 1 °C. The transition points of C-H, C=O groups in N-20 can be determined to be *ca.* 38 °C, and the thermal transition generally located in between 35 and 42 °C. It appears that all the groups in the N-20 responds slower to the temperature change than that in the precursors, which may be caused by the cross-linked network architecture of the nanogels.

## **Introduction to 2Dcos**

2Dcos is a mathematical method, whose basic principles were proposed first by Noda.<sup>6</sup> It has been widely applied to study spectral variations of different chemical groups that respond to external perturbations, *i.e.*, temperature, pH, concentration, electromagnetic and so on.<sup>7</sup> Through spreading the original spectra along a second dimension, it can extract additional important information about conformational changes or molecular motions, which are not easily obtained from the conventional IR spectra.

The 2Dcos spectra are characterized by two independent wavenumber axes ( $\nu_1$ ,  $\nu_2$ ) and a correlation intensity axis. Two types of spectra, 2D synchronous and asynchronous spectrum are obtained generally. The correlation intensity in the 2D synchronous and asynchronous maps represents the relative degree of in-phase and out-of-phase response, respectively. The 2D synchronous spectra are symmetric in relation to the diagonal in the correlation map. Some peaks appearing along the diagonal are called auto-peaks, and the symbols of them are always positive, as auto-peaks reflect the degree of autocorrelation of perturbation-induced molecular vibrations. Where the auto-peak appears, the peak at this wavenumber would change greatly under environmental perturbation. 2D asynchronous spectra can not only enhance spectral resolution but also identify the specific order occurring in the effect of external perturbation as well. The judging rule can be extracted from Noda's rule.<sup>8</sup> In brief, when the cross-peaks ( $\nu_1, \nu_2$ , and assume  $\nu_1 > \nu_2$ ) in synchronous and asynchronous spectra possess the same symbol, it indicates the variation at  $\nu_1$  prior to that of  $\nu_2$ , and vice versa.

## Variable-temperature <sup>1</sup>H NMR Analysis

Variable-temperature <sup>1</sup>H NMR analysis was used to follow the solution behavior using the N-20 nanogels as the example. The peaks attributed to N-20 displayed an intensity reduction upon heating, suggesting the occurrence of collapse of the nanogels during their phase transitions (Figure S5a). To quantitatively characterize the phase transitions of the N-20, the phase transition fraction  $p$  was defined as  $p = 1 - (I/I_0)$ , where  $I$  is the integrated intensity of the given polymer signal in the spectrum of the partly separated system, and  $I_0$  is the integrated intensity of this signal when no phase separation occurs.<sup>9</sup> We take the integrated intensities obtained for the D<sub>2</sub>O solution at 25 °C for N-20 as  $I_0$ . The PEGA, MEA and PDS units in the nanogels cooperatively participate in the discontinuous phase transition process with a turning point at 39 °C, which is in line with the FTIR analysis (Figure S5b).

1. Zhou, W.; Qu, Q.; Xu, Y.; An, Z., *Acs Macro Lett.* **2015**, *4* (5), 495-499.
2. Sun, W.; An, Z.; Wu, P., *Macromol. Rapid Commun.* **2017**, *38* (9),1600808.
3. Kavimandan, N. J.; Losi, E.; Wilson, J. J.; Brodbelt, J. S.; Peppas, N. A., *Bioconjugate Chem.* **2006**, *17* (6), 1376-1384.
4. Thomas, M.; Richardson, H. H., *Vibr. Spectrosc.* **2000**, *24* (1), 137-146.
5. Morita, S.; Shinzawa, H.; Noda, I.; Ozaki, Y., *Appl. Spectrosc.* **2006**, *60* (4), 398-406.
6. Noda, I., *J. Am. Chem. Soc.* **1989**, *111* (21), 8116-8118.
7. Noda, I., *J. Mol. Struct.* **2008**, *883*, 2-26.

8. Noda, I., *Appl. Spectrosc.* **2000**, *54* (7), 994-999.
9. Starovoytova, L.; Spevacek, J.; Ilavsky, M., *Polymer* **2005**, *46* (3), 677-683.
10. Hou, L.; Wu, P., *Phys. Chem. Chem. Phys.* **2016**, *18* (23), 15593-15601.
11. Hou, L.; Ma, K.; An, Z.; Wu, P., *Macromolecules* **2014**, *47* (3), 1144-1154.
12. Zhang, B.; Tang, H.; Wu, P., *Macromolecules* **2014**, *47* (14), 4728-4737.

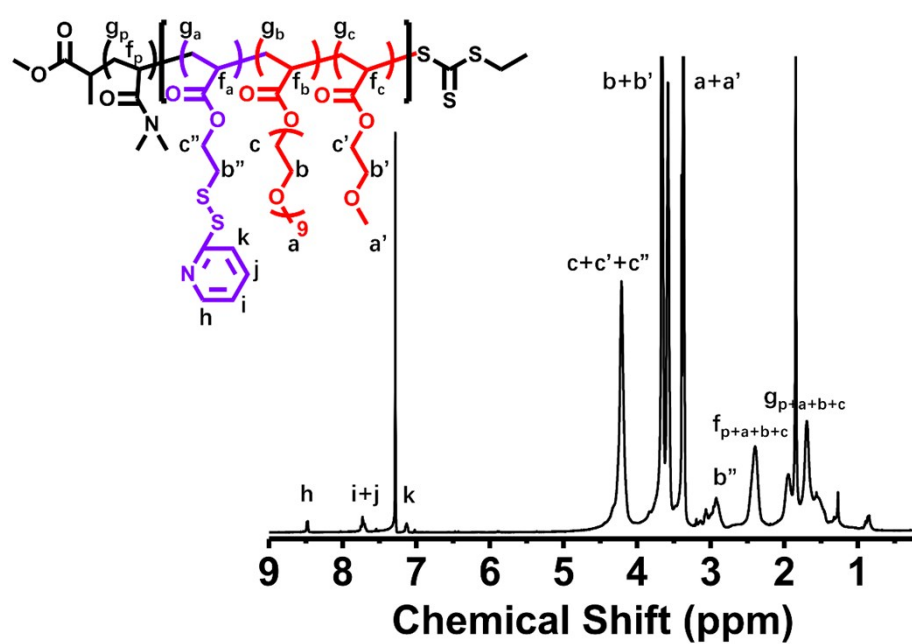


**Figure S1.**  $^1\text{H}$ NMR spectrum of the precursor polymer in  $\text{CDCl}_3$ .

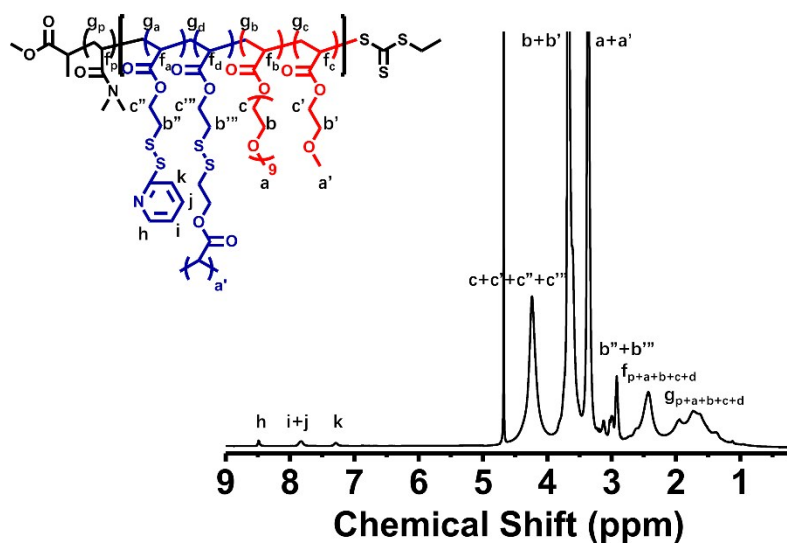


Figure S2.  $^1\text{H}$ NMR spectrum of the N-20 nanogels in  $\text{D}_2\text{O}$ .

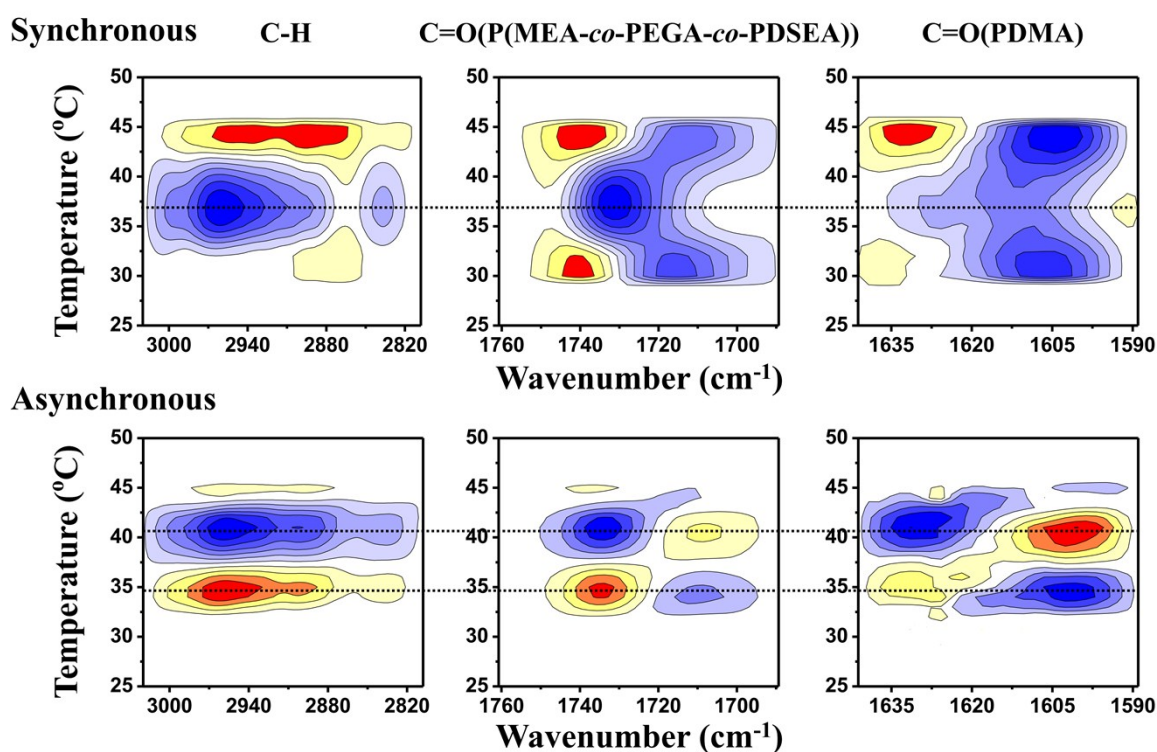
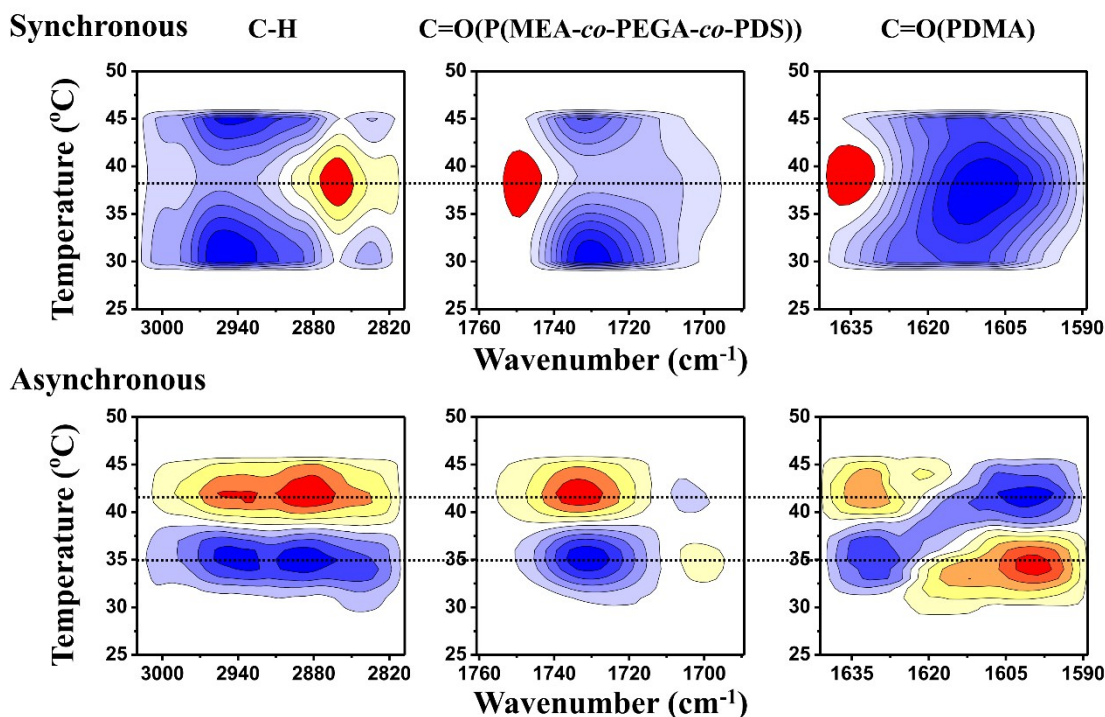


Figure S3. PCMW synchronous and asynchronous spectra of PDMA-b-P(MEA-co-PEGA-co-PDSEA) polymers during heating from 25 to 50 °C, respectively. Herein, warm colors

(red and yellow) represent positive intensities, while cool colors (blue) negative ones.



**Figure S4.** PCMW synchronous and asynchronous spectra of P(MEA-*co*-PEGA-*co*-PDS)/PDMA nanogels during heating from 25 to 50 °C, respectively. Herein, warm colors (red and yellow) represent positive intensities, while cool colors (blue) negative ones.

**Table S1.** Tentative band assignments of PDMA-*b*-P(MEA-*co*-PEGA-*co*-PDSEA) polymers in D<sub>2</sub>O according to the 2Dcos analysis.<sup>10-12</sup>

Wavenumber (cm <sup>-1</sup> )	Tentative Assignments
3003	$\nu_{\text{as}}(\text{CH}_3)(-\text{OCH}_3)(\text{hydrated})$
2983	$\nu_{\text{as}}(\text{CH}_3)(-\text{OCH}_3)(\text{dehydrated})$
2968	$\nu_{\text{as}}(\text{CH}_2)(-\text{OCH}_2\text{CH}_2\text{O}-)(\text{hydrated})$
2960	$\nu_{\text{as}}(\text{CH}_2)(-\text{OCH}_2\text{CH}_2\text{O}-)(\text{dehydrated})$
2956	$\nu_{\text{as}}(\text{CH}_2)(-\text{OCH}_2\text{CH}_2\text{-S-S-})(\text{hydrated})$
2949	$\nu_{\text{as}}(\text{CH}_2)(-\text{OCH}_2\text{CH}_2\text{-S-S-})(\text{dehydrated})$
2895	$\nu_{\text{s}}(\text{CH}_3)(-\text{OCH}_3)(\text{hydrated})$
2868	$\nu_{\text{s}}(\text{CH}_3)(-\text{OCH}_3)(\text{dehydrated})$
2837	$\nu_{\text{s}}(\text{CH}_2)(-\text{OCH}_2\text{CH}_2\text{O}-)(\text{hydrated})$
2821	$\nu_{\text{s}}(\text{CH}_2)(-\text{OCH}_2\text{CH}_2\text{O}-)(\text{dehydrated})$
1745	$\nu(\text{C=O})(\text{dehydrated})(\text{P(MEA-}i{co}\text{-PEGA-}i{co}\text{-PDSEA)})$

**Table S2.** Tentative band assignments of P(MEA-*co*-PEGA-*co*-PDSEA)/PDMA nanogels in D<sub>2</sub>O according to the 2Dcos analysis. <sup>10-12</sup>

Wavenumber (cm <sup>-1</sup> )	Tentative Assignments
3005	$\nu_{\text{as}}(\text{CH}_3)(-\text{OCH}_3)(\text{hydrated})$
2987	$\nu_{\text{as}}(\text{CH}_3)(-\text{OCH}_3)(\text{dehydrated})$
2964	$\nu_{\text{as}}(\text{CH}_2)(-\text{OCH}_2\text{CH}_2\text{O}-)(\text{hydrated})$
2953	$\nu_{\text{as}}(\text{CH}_2)(-\text{OCH}_2\text{CH}_2\text{O}-)(\text{dehydrated})$
2947	$\nu_{\text{as}}(\text{CH}_2)(-\text{OCH}_2\text{CH}_2\text{-S-S-})(\text{hydrated})$
2941	$\nu_{\text{as}}(\text{CH}_2)(-\text{OCH}_2\text{CH}_2\text{-S-S-})(\text{dehydrated})$
2877	$\nu(\text{CH})(\text{backbone})$
2839	$\nu_{\text{s}}(\text{CH}_2)(-\text{OCH}_2\text{CH}_2\text{O}-)(\text{hydrated})$
2818	$\nu_{\text{s}}(\text{CH}_2)(-\text{OCH}_2\text{CH}_2\text{O}-)(\text{dehydrated})$
1751	$\nu(\text{C}=\text{O})(\text{dehydrated})(\text{P}(\text{MEA-}i{co}\text{-PEGA-}i{co}\text{-PDS}))$
1736,1724	$\nu(\text{C}=\text{O})(\text{dehydrating})(\text{P}(\text{MEA-}i{co}\text{-PEGA-}i{co}\text{-PDS}))$
1703	$\nu(\text{C}=\text{O})(\text{hydrated})(\text{P}(\text{MEA-}i{co}\text{-PEGA-}i{co}\text{-PDS}))$
1630	$\nu(\text{C}=\text{O})(\text{dehydrated})(\text{PDMA})$
1608	$\nu(\text{C}=\text{O})(\text{hydrated})(\text{PDMA})$

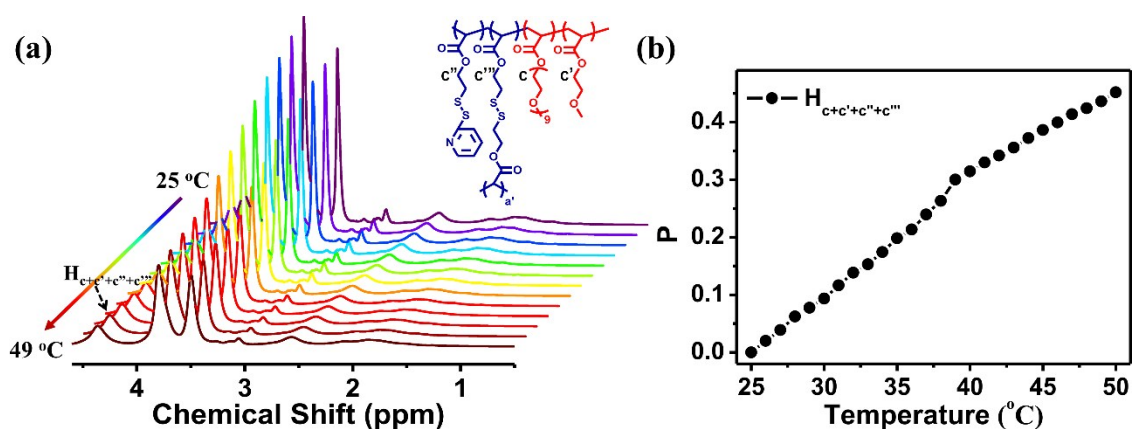


**Figure S5.** (a) variable-temperature <sup>1</sup>H NMR spectra of N-20 upon heating and (b) temperature dependence of phase separation fraction *p* for protons of N-20 from 25 to 50 °C.